ANALYTICAL BIOCHEMISTRY **244,** 86–95 (1997)
ARTICLE NO. AB969879

Fluorescence Properties of Pteridine Nucleoside Analogs as Monomers and Incorporated into Oligonucleotides

Mary E. Hawkins,* Wolfgang Pfleiderer,† Frank M. Balis,* Denise Porter,‡ and Jay R. Knutson‡
**Pediatric Branch, National Cancer Institute, and ‡National Heart Lung and Blood Institute, NIH, Bethesda, Maryland 20892-1928; and †Fakultät für Chemie, Universität Konstanz, Konstanz, Germany*

Received August 22, 1996

Eighteen fluorescent pteridine-based nucleoside analogs have been prepared that are suitable for synthesis as phosphoramidites and site-specific incorporation into oligonucleotides. Their quantum yields ranged from ⩽0.03 to 0.88. The maximum excitation and emission wavelengths of seven selected probes with quantum yields >0.15 ranged from 334 to 358 and 400 to 444 nm, respectively. Fluorescence decay curves of the seven probes were biexponential, and the mean intensity-weighted lifetimes ranged from 0.87 to 6.54 ns. Incorporation of probes 4 and 17 (3-methylisoxanthopterin and 6-methylisoxanthopterin) into oligonucleotides significantly quenched their fluorescence signal, and the degree of quench correlated with the number and proximity of purines in the oligonucleotide. Incorporation also resulted in a shift in absorbance-, emission-, and decay-associated spectra for 6-methylisoxanthopterin. An increase in the complexity of the decay curve and a decrease in the mean lifetime occurred for both probes. Formation of double-stranded oligonucleotides did not substantially increase the degree of quenching but generally increased the complexity of decay curves and decreased the mean lifetimes. Melting temperature, T_m, depression equivalent to that of a single base pair mismatch was observed in 3-methylisoxanthopterin-containing double-stranded oligonucleotides, while the T_m of 6-methylisoxanthopterin-containing double-stranded oligonucleotides were unperturbed, e.g., equivalent to unlabeled double-stranded oligonucleotides. This new class of fluorophore yields promising probes for the study of protein/DNA interactions.

Fluorescence is an extremely useful tool for studying protein/DNA interactions. Fluorescence properties can be exquisitely sensitive to changes in the physical and chemical environment and can be used to characterize dynamic properties (e.g., rotational diffusion and complex formation) of macromolecules to which they are attached. Changes in pH, interaction with other molecules, or alterations in tertiary structure may result in changes in fluorescence intensity, lifetime of fluorescence emission, or fluorescence depolarization; similarly, they may cause a shift in the emission, excitation, or absorption spectra of the fluorophore. Measuring these properties can provide information about the kinetics of macromolecular interactions, changes in structure, and enzymatic reactions.

Most traditional DNA probes are bulky molecules attached through a carbon linker, leaving them free to move in ways that may be independent of the complex to which they are attached. Efforts to identify "quasi intrinsic" probes, i.e., fluorescent molecules that are structural analogs of the endogenous subunits of DNA, have led to development of etheno-substituted nucleoside analogs (1) and 2-aminopurine (2–6). These fluorophores can be substituted for endogenous nucleotides and have proven useful for investigations of DNA structure and DNA/protein interactions (3, 7–9). Incorporation of a fluorescent nucleoside analog through the normal phosphodiester linkage should restrict the fluorophore's independent movement, and measurements of anisotropy (8) or intensity changes from such probes should more accurately reflect DNA interactions and movement.

Ideally, a fluorescent nucleoside analog should closely resemble the naturally occurring purine or pyrimidine base structure, especially at hydrogen bonding sites critical to base pairing. The fluorophore should be available as a phosphoramidite to allow site-specific insertion with automated DNA synthesizers. It should also have reasonable fluorescence under physiologically relevant conditions (e.g., aqueous buffer, pH 6 to 8). Finally, the fluorophore's disruption of sequence

0003-2697/97 $25.00

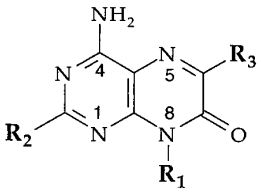

Probe	R_1	R_2	R_3
1	Ribose		−H
2	Ribose	−H	
25	Deoxyribose	−H	−H

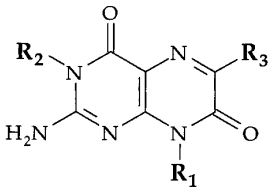

Probe	R_1	R_2	R_3
4	Ribose	$-CH_3$	−H
5	Ribose	−H	−H
17	Deoxyribose	−H	$-CH_3$

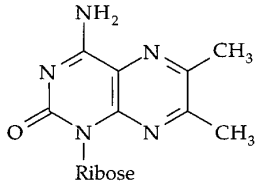

Probe 10

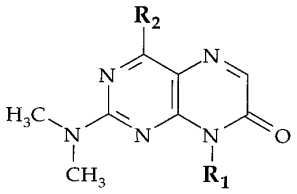

Probe	R_1	R_2
3	Ribose	OCH_2 
6	Deoxyribose	−H

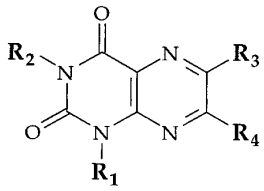

Probe	R_1	R_2	R_3	R_4
7	Ribose	−H		−H
8	Ribose	−H	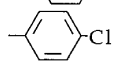 Cl	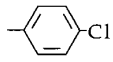 Cl
9	Ribose	−H	$-CH_3$	$-CH_3$
12	Deoxyribose	−H	−H	−H
13	−H	Ribose	−H	−H
14	−H	Ribose		
16	Ribose	−H		

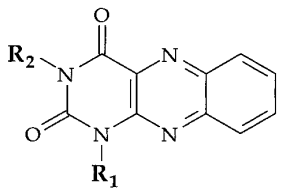

Probe	R_1	R_2
11	Ribose	−H
15	−H	Ribose

FIG. 1. Chemical structures of the 18 pteridine nucleoside analogs. Compounds are grouped according to similarities in their chemical structures. The seven pteridine compounds in the top row were selected for more detailed study based on their favorable Q_{rel}.

recognition critical to protein/DNA interactions should be minimal.

Pteridines are a class of bicyclic planar compounds, some of which are highly fluorescent and structurally similar to purines. We characterized the fluorescence properties of selected pteridine nucleoside analogs. These included two compounds that were synthesized in dimethoxytrityl phosphoramidite form and incorporated into oligonucleotides. Fluorescence characteristics of pteridine-labeled oligonucleotides were studied in single- and double-stranded forms.

MATERIALS AND METHODS

Chemicals. The solubility, fluorescence intensity, and structural similarity to endogenous nucleosides was assessed for 18 pteridines, and 7 compounds were selected for more intensive study (Fig. 1). The synthetic pathways of most of the selected fluorophores have been previously reported (probes 1 and 2 (10), probe 3 (11), probe 4 (12), probe 5 (13), probe 8 (14), probe 9 (15), probe 11 (16), probe 12 (17), probe 13 and 14 (18), probe 15 (19), probe 16 (15)). Synthesis of probes 6, 7, 10, 17, and 25 will be reported elsewhere. Fourteen probes were initially studied in the ribopteridine form (ribonucleoside analog) and four probes were studied as deoxyribopteridines (deoxyribonucleoside analogs). The ribose or deoxyribose was attached at position 1, 3, or 8 on the pteridine ring (Fig. 1). The phosphoramidite form of probe 4 (3-methyl-8-(2-deoxy-5-*O*-dimethoxytrityl-β-D-ribofuranosyl)isoxanthopterin-3′-*O*-(β-cyanoethyl, *N*-diisopropyl)phosphoramidite) was synthesized as previously described (20). Synthesis of the phosphoramidite of probe 17 will be published separately.

Using the phosphoramidite forms of the fluoro-

TABLE 1

Oligonucleotide Sequences into Which Probes 4 and 17 Were Incorporated

Name	
PTER1	5′- GT**F** TGG AAA ATC TCT AGC AGT -3′
PTER2	5′- GTG T**F**G AAA ATC TCT AGC AGT -3′
PTER3	5′- GTG TG**F** AAA ATC TCT AGC AGT -3′
PTER4	5′- GTG TGG AAA ATC TCT A**F**C AGT -3′
PTER5	5′- GTG TGG AAA ATC TCT AGC A**F**T -3′
PTER7	5′- ACT GCT AGA **F**AT TTT CCA CAC -3′
PTER8	5′- ACT GCT A**F**A GAT TTT CCA CAC -3′
PTER9	5′- ACT **F**CT AGA GAT TTT CCA CAC -3′

Note. **F** designates the location at which the probe is incorporated. PTER1–5 have a sequence that is complementary to the sequence of PTER7–9.

phores, we incorporated them directly into oligonucleotides using an Applied Biosystems Model 392 (Foster City, CA) automated DNA synthesizer following standard protocols recommended by the manufacturer. Details of the synthesis and purification have been reported previously (20). Sequences of the oligonucleotides containing either probe 4 or probe 17 are shown in Table 1.

We demonstrated a relationship between the degree of quench and the proximity to other purine nucleobases in the strand. Maximum quench was observed with purines immediately adjacent to the fluorophore. Purines in the second neighboring position also appear to quench the fluorescence signal. Relative quantum yields were confirmed by measuring the ratio of fluorescence of a single strand containing the probe and that of the total digest of that strand using P1 nuclease. These ratios agreed with those of measured quantum yields of single strand and monomer.

Spectroscopic analysis. Q_{rel} were measured on an SLM Model 8000 (SLM Instruments, Urbana, IL) spectrofluorometer with a 450-W xenon arc lamp as the light source. The spectrofluorometer was interfaced to an SPEX 386 computer (SPEX Industries, Edison, NJ). Q_{rel} measurements were performed on samples with optical densities $\leqslant 0.12$ at the excitation wavelength in 10 mM Tris·Cl, pH 7.5, at room temperature using 1 $\times$ 1-cm quartz cuvettes. The excitation wavelength was 360 or 310 nm and the fluorescence emission was measured at 440 or 460 nm. Corrected emission spectra were integrated and referenced to quinine sulfate (quantum yield 0.51). A correction factor for emission spectra was derived by comparison of the published emission spectrum of quinine sulfate (21) to the quinine sulfate emission spectrum collected on the SLM spectrofluorometer using identical concentration and solvent. Excitation spectra corrected for the wavelength-dependent intensity of the exciting light were obtained using the quantum counter (concentrated rhodamine in ethylene glycol) in the reference channel (22). The effect of pH on the emission spectra of probes 4 and 17 was measured in 10 mM Tris·Cl over the pH range from 5.0 to 9.5 in half pH unit increments.

Lifetimes were obtained by fitting a multiexponential model to time-correlated single photon counting decay data, using a weighted nonlinear least-squares method (23). Goodness of fit was assessed with the χ^2 function (24). For decay-associated spectra (DAS)[1] time-resolved data were obtained on samples by excitation at 330 nm and observation every 5 nm over the emission band. The excitation pulse ("lamp") profile was obtained with a light-scattering suspension (Ludox) from Sigma. Further instrumentation details were as previously described (25, 26).

Data analysis routinely included deconvolution for the excitation pulse, which had an instrumental halfwidth of 800 ps (26). A convolved multiexponential model, $I'(t)$, describing the time course of fluorescence intensities (Eq. [1]) was fit to the fluorescence decay data

$$I'(t) = \int L(t')I(t' - t)dt', \qquad [1]$$

where $L(t)$ is the lamp function (response of the instrument to the test laser pulse and

$$I(t) = \sum_{i=1}^{n} \alpha_i e^{(-t/\tau_i)}, \qquad [2]$$

where $I(t)$ is the fluorescence intensity, α_i are the preexponentials, and τ_i are the lifetimes. Total fluorescence intensity, $I = \Sigma_{i=1}^{n} \alpha_i\tau_i$, and the percentage intensity from each component of the multiexponential model is $\%I_i = \alpha_i\tau_i/I \times 100$. Mean lifetimes (intensity weighted lifetime, τ_m) and the species-concentration-weighted lifetime $\langle\tau\rangle$ are defined as:

$$\tau_m = \frac{\Sigma_{i=1}^{n} \alpha_i\tau_i^2}{\Sigma_{i=1}^{n} \alpha_i\tau_i} \qquad [3]$$

and

$$\langle\tau\rangle = \frac{\Sigma_{i=1}^{n} \alpha_i\tau_i}{\Sigma_{i=1}^{n} \alpha_i}. \qquad [4]$$

The degree of departure from monoexponential decay can be assessed by comparing relative magnitudes of

[1] Abbreviation used: DAS, decay-associated spectra.

the preexponentials (α_i), the percentage contribution to the intensity (I_i) of each component, and the difference between τ_m and $\langle\tau\rangle$. When a decay is made up of components differing greatly in lifetime, τ_m will be much longer than $\langle\tau\rangle$.

In complex systems, DAS are the emission spectra that belong to each lifetime obtained from fluorescence decay surfaces (25). DAS are used to dissect the heterogeneity of the emission but do not, in themselves, specify its origin. The lifetimes were obtained by global analysis of the entire surface. The DAS can then be viewed as plots of the preexponential constants (α_i) at each wavelength, and these spectra can be normalized to provide the intensity contribution from each component.

To gain insight into the mechanisms of quenching when the pteridines are inserted into an oligonucleotide, we evaluated the relationship between quantum yield and lifetimes. In pure dynamic quenching (quenching events occurring during the excited state) where quenching competes with fluorescence,

$$Q = \frac{\tau}{\tau_n}, \qquad [5]$$

where Q is the quantum yield, τ is the measured lifetime, and τ_n is the natural, or radiative, lifetime (i.e., one that would be observed for $Q = 1$). Deviations from Eq. [5] such that $\tau/Q > \tau_n$ signify static (or quasistatic) quenching (27 and references therein), which in turn is usually due to ground-state formation of nonfluorescent complexes. Equation [5] is therefore a guide to whether a quenching mechanism operates predominantly in the excited or ground state. When applied to a heterogeneous solution, Eq. [5] may be modified to use a mean lifetime that is the sum of the contributions from each component, namely $\langle\tau\rangle$ (27).

Spectrophotometric absorbance measurements were made on a Hewlett–Packard Model 8452a spectrophotometer (Palo Alto, CA).

Melting temperatures. Melting temperature of double-stranded oligonucleotides was measured by monitoring absorbance hyperchromicity at 260 nm in a Hewlett–Packard Model 8452a spectrophotometer equipped with a Hewlett–Packard 89090A Peltier temperature controller. Samples were measured in 10 mM Tris, pH 7.5, with a NaCl concentration of 10 mM. Temperature was increased by 1°C per minute with a 1-min equilibration time between increments.

RESULTS

Fluorescence of ribo- and deoxyribopteridines. We measured the Q_{rel} of the 18 ribo- and deoxyribopteridine compounds shown in Fig. 1. For probes 3, 6, 7–9, and 11–16, the Q_{rel} was <0.03, so the fluorescence properties of these compounds were not further characterized. The remaining probes (1, 2, 4, 5, 10, 17, and 25) were highly fluorescent. Q_{rel} of these probes ranged from 0.16 to 0.88 (Table 2). The overlaid absorption spectra, corrected excitation spectra, and emission spectra of these seven selected probes are shown in Fig. 2, and Table 2 lists the fluorescence properties for these compounds, including the lifetime/quantum yield ratios expressed as both τ_m/Q_{rel} and $\langle\tau\rangle/Q_{rel}$.

The fluorescent pteridine nucleoside analogs are grouped in Table 2 according to the structural similarities shown in Fig. 1. Probes 1, 2, and 25 have a 4-amino-7-oxo configuration and differ by the presence and placement of a phenyl group. This series of compounds could be considered adenosine analogs. The Q_{rel} of these probes is lower (0.16 to 0.41) than that of other selected probes, even in the absence of the substituted phenyl group (probe 25). Probe 2 (6-phenyl substituted) has the lowest Q_{rel} and shortest mean lifetime. Probes 4, 5, and 17 (2-amino-4,7-oxo derivatives) are considered guanosine analogs and differ only by presence and placement of a methyl group. These probes exhibit similar Q_{rel} (0.70 to 0.88) and mean lifetimes (τ_m ranges from 5.63 to 6.54 ns). Probe 10 is the 2-oxo-4-amino-6,7-methyl-substituted probe and it has a Q_{rel} of 0.54 and a mean lifetime (τ_m) of 3.52 ns.

Effect of pH on fluorescence emission. Emission spectra of probes 4 and 17 over a pH range from 5.0 to 8.0 are shown in Fig. 3. Varying the pH had no effect on the emission spectrum of probe 4, whereas the emission spectrum of probe 17 shifted 10 nm to the red when the pH was increased from 7.0 to 8.0. A similar pH titration of DAS for probes 4 and 17 was performed. The lifetime components for probe 4 remained unchanged over the pH range from 7.0 to pH 9.0, while with probe 17, there is a blue shift in the longest lived DAS and a smaller increase in the shorter lived component. These DAS demonstrate a pH-dependent equilibrium between a minimum of two emitting species (Fig. 4).

Fluorescence of fluorophore-containing oligonucleotides. Probes 4 (3-methylisoxanthopterin) and 17 (6-methylisoxanthopterin) were incorporated into the oligonucleotide strands shown in Table 1 and examined in single- and double-stranded forms (paired to cytidine in the complementary strand). We previously reported relative quantum yields (Q_{rel}) measurements of probe 4-containing oligonucleotides (21-mer) in which the fluorophore was substituted for guanosine at several positions (20). Fluorescence properties of the fluorophore-containing oligonucleotides are presented in Table 3. In PTER8 the fluorophores were inserted into a purine-rich segment of the oligonucleotide and fluorescence of both probes was substantially quenched,

TABLE 2

Fluorescence Properties of the Pteridine Nucleoside Analogs

Probe	Ex_{max}[a] (nm)	Em_{max} (nm)	Q_{rel}	τ_i (ns)	α_i	$\%I_i$ (%)	τ_m (ns)	$\langle\tau\rangle$ (ns)	τ_m/Q_{rel} (ns)	$\langle\tau\rangle/Q_{rel}$ (ns)
1	354	444	0.41	$\tau_1 = 1.91$	$\alpha_1 = 0.19$	$\%I_1 = 9.9$	3.84	3.64	9.36	8.88
				$\tau_2 = 4.05$	$\alpha_2 = 0.81$	$\%I_2 = 90.1$				
2	358	440	0.16	$\tau_1 = 0.76$	$\alpha_1 = 0.67$	$\%I_1 = 59.6$	0.87	0.85	5.31	5.31
				$\tau_2 = 1.05$	$\alpha_2 = 0.33$	$\%I_2 = 40.4$				
25	334	443	0.27	$\tau_1 = 2.37$	$\alpha_1 = 0.19$	$\%I_1 = 11.6$	3.92	3.80	14.52	14.07
				$\tau_2 = 4.13$	$\alpha_2 = 0.81$	$\%I_2 = 88.4$				
4	348	430	0.88	$\tau_1 = 3.54$	$\alpha_1 = 0.02$	$\%I_1 = 1.2$	6.54	6.51	7.40	7.40
				$\tau_2 = 6.58$	$\alpha_2 = 0.98$	$\%I_2 = 98.8$				
5	348	430	0.87	$\tau_1 = 1.81$	$\alpha_1 = 0.37$	$\%I_1 = 14.6$	5.63	4.65	6.71	7.04
				$\tau_2 = 6.26$	$\alpha_2 = 0.63$	$\%I_2 = 85.4$				
17	340	431	0.70	$\tau_1 = 5.45$	$\alpha_1 = 0.20$	$\%I_1 = 17.5$	6.38	6.35	9.11	9.07
				$\tau_2 = 6.58$	$\alpha_2 = 0.80$	$\%I_2 = 82.5$				
10	336	400	0.54	$\tau_1 = 3.16$	$\alpha_1 = 0.97$	$\%I_1 = 92.8$	3.52	3.31	6.52	6.13
				$\tau_2 = 8.14$	$\alpha_2 = 0.03$	$\%I_2 = 7.2$				

Note. Measurements were taken in 10 mM Tris buffer, pH 7.5, at room temperature.

[a] Abbreviations: Ex_{max}, excitation wavelength maximum, EM_{max}, emission wavelength maximum; Q_{rel}, relative quantum yield; τ_i, lifetime for each component of a multiexponential model; α_i, preexponential for each component of a multiexponential model; $\%I_i$, percentage fluorescence intensity for each component of a multiexponential model; $\langle\tau\rangle$, species-concentration-weighted lifetime; τ_m, intensity-weighted lifetime.

whereas in PTER9 the fluorophores are surrounded by pyrimidines resulting in less quenching of the fluorescence signal.

With probe 4, double-strand formation led to no substantial increase in quench over that seen in the single-stranded oligonucleotide (Table 3, Fig. 5). In the PTER9 oligonucleotide, the degree of quench relative to the unincorporated probe 4 was 64 and 68% in the single- and double-stranded forms, respectively. For probe 17, the degree of quench in PTER9 increased from 56 to 64% on going from the single- to the double-stranded form. The emission spectrum of probe 17 shifts 7 nm to the red when it is incorporated into a single- or double-stranded oligonucleotide compared to its unincorporated monomer form. The emission spectrum of probe 4 shifts only 2 nm when incorporated into an oligonucleotide.

The lifetimes, mean lifetimes, and amplitudes for probes 4 and 17 incorporated into single-stranded and double-stranded oligonucleotides are listed in Table 3. The dominant component of the intensity decay curve for probes 4 and 17 has a lifetime of 6.58 and 6.26 ns, respectively, but when these fluorophores are incorporated into an oligonucleotide, the decay curves become more complex and components of the decay curve with shorter lifetimes become more prominent. For example, probe 4 in PTER8 has a triexponential decay curve with the predominant component having a lifetime of 0.21 ns.

Melting temperatures. Melting temperatures (T_m) were measured on a series of fluorophore-containing oligonucleotides as well as on the identical strands containing no fluorophore and strands containing a 1-bp mismatch at the identical position to the fluorophores (Table 4). For probe 4-containing oligonucleotides, T_m depression was approximately equivalent to a single base-pair mismatch at the identical position. The T_m's of probe 17-containing oligonucleotides were not depressed compared with the identical oligonucleotide containing no fluorophore (Table 4).

DISCUSSION

From a series of substituted pteridine nucleoside analogs, we have identified several compounds which are highly fluorescent, and which can be synthesized as phosphoramidites and incorporated into DNA oligonucleotides (probes 4 and 17) through the normal phosphodiester linkage using a standard DNA synthesizer. Although incorporation into DNA significantly quenches the fluorescence signal, the selected fluorophores start with quantum yields as high as 0.88 and can still be easily detected within oligonucleotides. Changes in the local structure of fluorophore-containing oligonucleotides can be monitored by measuring changes in fluorescence properties, as we previously demonstrated in an assay for the HIV integrase cleavage reaction. In the integrase assay, a dinucleotide containing the fluorophore is cleaved from the 3′-end of the oligonucleotide resulting in a marked increase in fluorescence intensity. Other protein/DNA interactions which disrupt the tertiary structure of DNA could also be expected to alter fluorescence properties.

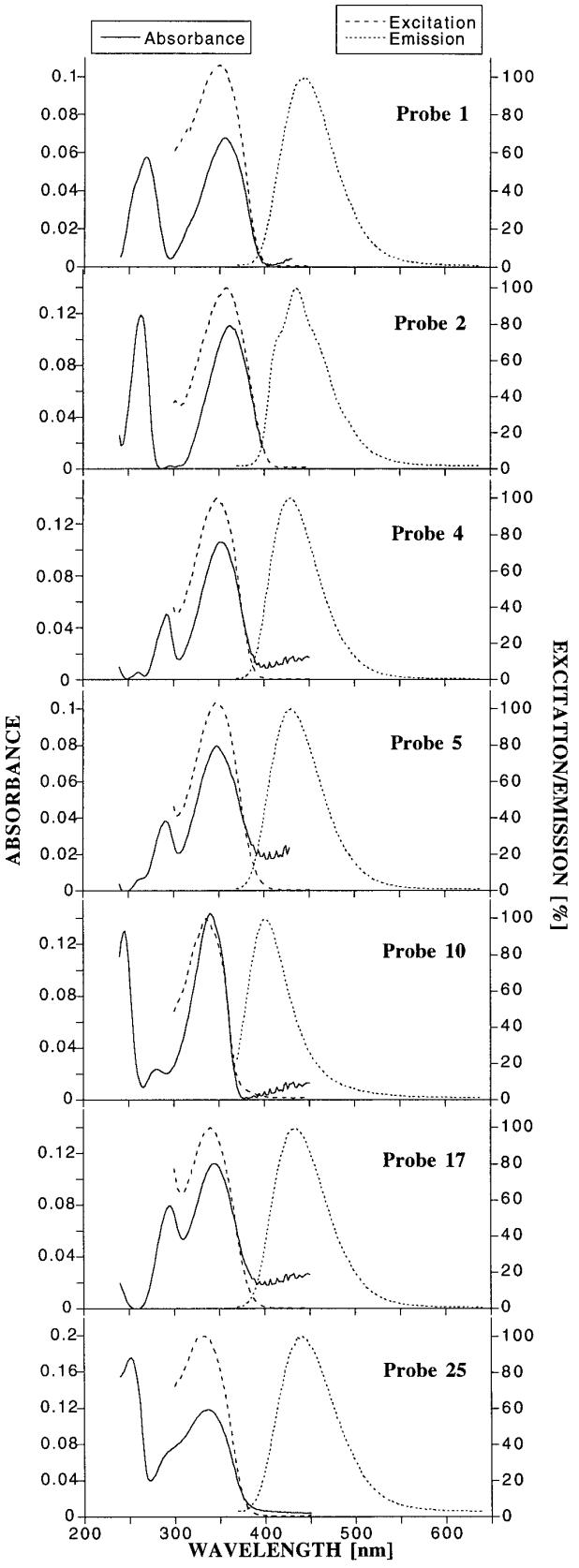

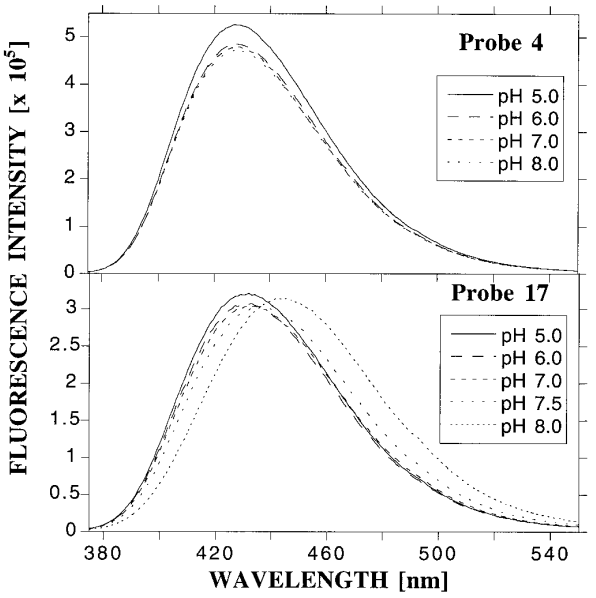

FIG. 3. Emission spectra of probe 4 (A) and probe 17 (B) at pH 5.0, 6.0, 7.0, 7.5, and 8.0.

Probes 4, 5, and 17 have the highest relative quantum yields (0.70–0.88) and bear a structural resemblance to guanosine, whereas probes 1, 2, and 25 have somewhat lower quantum yields (0.16–0.41) and are adenosine analogs. Each of the selected pteridine nucleoside analogs with high quantum yield (probes 1, 2, 4, 5, 10, 17, and 25) has an amino group at either the 2- or 4-position. Probes 4, 5, and 17 differ only in the presence or position of a methyl group, and their spectral properties (Fig. 2) and quantum yields are very similar. Probes 1, 2, and 25 differ only in the presence and position of a phenyl group which leads to lower yield when in the 6-position than in the 2-position. Ribo- and deoxyribolumazine (probes 12 and 13) and the substituted derivatives of lumazine (probes 7, 8, 9, 11, 14, 15, 16), which have oxo groups at both the 2- and 4-positions, have surprisingly low quantum yields. This is in contrast to findings from studies conducted by J. Lee and A. Visser where 6,7-dimethyl-8-(1′-D-ribityl)lumazine has a fluorescence yield of 0.6 (28, 29). The only difference between this molecule and probe 9 in our study is the attachment of the sugar through the 1-position instead of the 8-position. Probe 10 is the only fluorophore with a high quantum yield and a sugar at the 1-position.

FIG. 2. Overlay of absorption spectra (—), corrected excitation spectra (---), and emission spectra (· · ·) for each of the seven selected probes. Excitation and emission are expressed as a percentage of maximum.

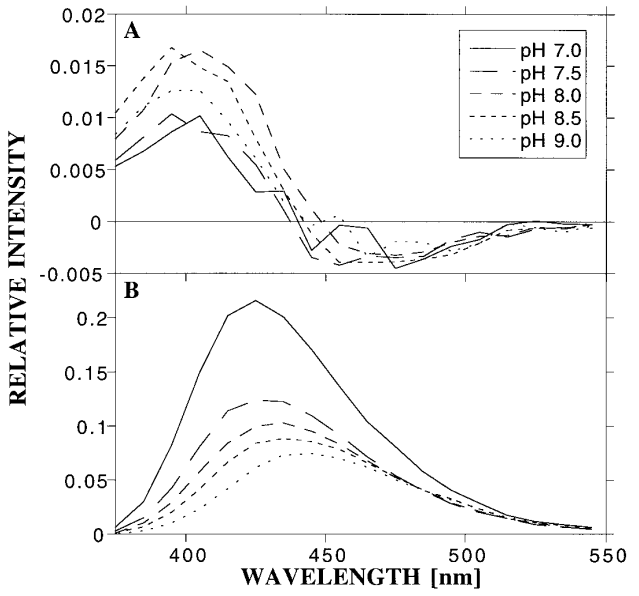

FIG. 4. Decay-associated spectra for probe 17 over a pH range of 7.0 to 9.0 for the ~3-ns lifetime (A) and the ~6-ns lifetime (B).

The significant quenching seen upon incorporation of probes 4 or 17 into single-stranded oligonucleotides is related to the proximity of purines to the fluorophores in the strand. This degree of quench is not substantially increased upon annealing the fluorophore-containing oligonucleotide to its complementery strand suggesting that quenching originates in base stacking interactions rather than base pairing. For PTER8 (where the fluorophore is surrounded by purines), the fluorescence signal is almost completely quenched (96%) in the single-stranded form, and no additional quench is detected in the double-stranded form. For PTER9 containing probe 17, quench increases from 56 to 64% with annealing, and for PTER9 containing probe 4, there is an even smaller increase in quench from 64 to 68% when the labeled strand is annealed to its complement.

The T_m studies suggest that probe 4 does not take part in base pairing in double-stranded oligonucleotides because the T_m depression in probe 4-containing oligonucleotides is approximately equivalent to that of a single base pair mismatch. In contrast, the T_m's of double-stranded probe 17-containing oligonucleotides are very similar to the T_m's of the controls, suggesting that probe 17 may participate in base pairing. The shift in emission spectra of probe 17 on going from single-stranded to double-stranded form is also consistent with base pairing. A shift of this type was not observed for double-stranded probe 4.

Lifetimes provide another means of monitoring the effects of quenchers or energy transfer interactions. For example, if a fluorophore within an oligonucleotide is shielded because of an interaction between the oligonucleotide and a protein, the lifetime will not be affected by the introduction of extrinsic dynamic quenchers (e.g., Cs^+ or I^-). However, if the probe is in a more exposed position within the oligonucleotide, then the lifetime will be affected by the addition of dynamic quenchers. Similarly, a probe may be dynamically quenched by collisions with intrinsic quenchers, e.g., neighboring groups such as carbonyl oxygen. Probe 2 has the shortest lifetime and the lowest quantum yield of all the selected probes. It appears that this probe is dynamically quenched compared to its cohorts; we have not yet discerned the quenching source.

In its monomer form, probe 4 has one major lifetime component of 6.58 ns (99%) and a $\langle\tau\rangle$ of 6.51 ns. Upon incorporation into PTER8, the decay curve becomes more complex and two distinct lifetimes of 2.35 ns (41%) and 6.06 ns (59%) are required to describe the decay curve, resulting in a $\langle\tau\rangle$ of 4.54 ns. Annealing this fluorophore-containing oligonucleotide to its complementery strand forming the double-stranded PTER8 increases the complexity even further, requiring a third, dominant short-lived component (0.21 ns) to fit the decay curve (Table 3), and the $\langle\tau\rangle$ drops to 1.45 ns. This latter change may provide a convenient means of monitoring whether an oligonucleotide (or a segment of an oligonucleotide) containing one of these fluorophores is in the single- or double-stranded state. In PTER9 the degree of quench associated with incorporation of probe 4 into the oligonucleotide is less, and there is no increase in the complexity of the decay curve and no substantial change in $\langle\tau\rangle$ in the double strand.

For probe 17, incorporation into PTER8 is also associated with substantial quenching, an increase in the complexity of the decay curve from two to three components, and a much shorter $\langle\tau\rangle$ (6.35 ns for the monomer and 0.95 ns in the single-stranded oligonucleotide). The double-stranded, probe 17-containing PTER8 oligonucleotide has a slightly shorter $\langle\tau\rangle$ (0.53 ns) than the single-stranded oligonucleotide. The change in the shape of probe 17's decay curve and the decrease in $\langle\tau\rangle$ resulting from annealing the fluorophore-containing single-stranded PTER9 to its complementery strand is more dramatic (Table 3). Based on the T_m measurements, probe 17 appears to participate in base-pairing interactions, while probe 4 does not. This may in part explain the differences in the observed changes in fluorescence properties of probe 4- and 17-containing oligonucleotides.

Comparing changes in $\langle\tau\rangle$ and relative quantum yield (expressed as percentage quench in Table 3) in the monomer and the fluorophore-containing single-

TABLE 3

Fluorescence Properties of the Pteridine Nucleoside-Containing Oligonucleotides

Probe	Sequence[a]	Strands[b]	Quench[c] (%)	τ_i[d] (ns)	α_i	$\%I_i$ (%)	τ_m (ns)	$\langle\tau\rangle$ (ns)
4	PTER8	Single	96	$\tau_1 = 2.35$	$\alpha_1 = 0.41$	$\%I_1 = 21.2$	5.27	4.54
				$\tau_2 = 6.06$	$\alpha_2 = 0.59$	$\%I_2 = 78.8$		
4	PTER8	Double	96	$\tau_1 = 0.21$	$\alpha_1 = 0.70$	$\%I_1 = 10.0$	4.60	1.45
				$\tau_2 = 2.88$	$\alpha_2 = 0.16$	$\%I_2 = 32.5$		
				$\tau_3 = 6.35$	$\alpha_3 = 0.13$	$\%I_3 = 57.5$		
4	PTER9	Single	64	$\tau_1 = 2.54$	$\alpha_1 = 0.31$	$\%I_1 = 17.8$	4.74	4.40
				$\tau_2 = 5.22$	$\alpha_2 = 0.69$	$\%I_2 = 82.2$		
4	PTER9	Double	68	$\tau_1 = 1.86$	$\alpha_1 = 0.33$	$\%I_1 = 14.5$	4.81	4.19
				$\tau_2 = 5.31$	$\alpha_2 = 0.67$	$\%I_2 = 85.4$		
17	PTER8	Single	96	$\tau_1 = 0.30$	$\alpha_1 = 0.81$	$\%I_1 = 25.6$	3.90	0.95
				$\tau_2 = 2.21$	$\alpha_2 = 0.14$	$\%I_2 = 31.3$		
				$\tau_3 = 7.28$	$\alpha_3 = 0.06$	$\%I_3 = 43.1$		
17	PTER8	Double	—	$\tau_1 = 0.21$	$\alpha_1 = 0.83$	$\%I_1 = 33.0$	2.59	0.53
				$\tau_2 = 1.20$	$\alpha_2 = 0.13$	$\%I_2 = 30.4$		
				$\tau_3 = 5.89$	$\alpha_3 = 0.03$	$\%I_3 = 36.6$		
17	PTER9	Single	56	$\tau_1 = 3.45$	$\alpha_1 = 0.25$	$\%I_1 = 14.1$	6.51	6.12
				$\tau_2 = 7.01$	$\alpha_2 = 0.75$	$\%I_2 = 85.9$		
17	PTER9	Double	64	$\tau_1 = 0.26$	$\alpha_1 = 0.88$	$\%I_1 = 43.4$	2.79	0.53
				$\tau_2 = 1.04$	$\alpha_2 = 0.09$	$\%I_2 = 17.0$		
				$\tau_3 = 6.30$	$\alpha_3 = 0.03$	$\%I_3 = 39.6$		

Note. Measurements were taken in 10 mM Tris buffer, pH 7.5, at room temperature.

[a] See Table 1 for oligonucleotide sequence and position of fluorophore within the oligonucleotide.

[b] Studies were performed on single-stranded fluorophore-containing oligonucleotide (single) and on the identical oligonucleotide annealed to its complementary strand (double).

[c] The degree of quench of the fluorescence emission relative to the deoxyribopteridine nucleoside analog (monomer). Quantum yields of probe 4 and 17 are listed in Table 2.

[d] Abbreviations: τ_i, lifetime for each component of a multiexponential model; α_i, preexponential for each component of a multiexponential model; $\%I_i$, percent fluorescence intensity for each component of a multiexponential model; $\langle\tau\rangle$, species-concentration-weighted lifetime; τ_m, intensity-weighted lifetime.

and double-stranded oligonucleotide provides insight into the mechanism of the quench resulting from incorporation of the pteridine nucleoside into an oligonucleotide. Static quench should not be accompanied by a change in $\langle\tau\rangle$, while pure dynamic quench is associated with proportional changes in quantum yield and $\langle\tau\rangle$. Disproportionate changes in quantum yield and $\langle\tau\rangle$ suggest that quenching is due to a combination of static and dynamic events. The tertiary structure of the oligonucleotide could expose the fluorophore to collisional events from its surroundings (dynamic quenching) or could position the fluorophore in contact with other bases or backbone quenchers within the oligonucleotide (static quenching). In the probe 4-containing PTER8 single-stranded oligonucleotide, the fluorophore is surrounded by purine bases and the Q_{rel} is 96% quenched compared with the monomer. The $\langle\tau\rangle$ of probe 4 is also shorter in the single-stranded oligonucleotide; but the change in $\langle\tau\rangle$ is only 30% (6.51 to 4.54 ns), suggesting that static quench arising from the surrounding purines is the primary mechanism involved in the quenching of the fluorescence signal.

The pH titration of the emission spectra and DAS of probes 4 and 17 yielded a shift in the emission spectrum of probe 17 between pH's 7.0 to 8.0 and an increase in one of probe 17's lifetime components over the pH range from 7.0 to 9.0. These DAS also provide a clear signature of an excited state reaction. (30) This property of probe 17 could be exploited to measure local pH and buffering. The shift in the emission spectrum of probe 17 was not seen with probe 4 and suggests that there is a protonation at the 3-position which is protected by the methyl group in probe 4. A minimum of two emitting species (e.g., tautomers) would be needed to explain these DAS.

These fluorophores may prove useful as sensitive tools for monitoring DNA interactions. The quenching of the fluorescence signal from within the oligonucleotide appears to be related to base stacking. Hence factors such as protein binding or enzymatic modifications

that alter the tertiary structure of DNA may result in changes in fluorescence of a vicinal probe. Another potential application of these fluorophores is in measurement of segmental motion via emission anisotropy. Measurement of changes in anisotropy provides insight into the "tightness" of binding to a particular segment of DNA (31). Since these fluorophores are incorporated directly into the DNA (unlike traditional linker arms) the changes in rotational motion associated with the interaction of the oligonucleotide with a protein should reflect those of normal DNA. This should permit mapping of the site of contact between a protein and a segment of DNA by placing a fluorophore in various positions.

These fluorophores also have a favorable spectral position, with absorption near 350 nm which overlaps well with the emission spectrum of tryptophan. In a fluorescence resonance energy transfer system, tryptophan, which emits near 350 nm, would be the donor and these fluorophores could serve as acceptors, if within ~30 Å of the tryptophan. The fluorophore would then respond with its own unique sensitized emission signal (32).

The potential advantages of this new class of fluorophores are their structural similarity to endogenous purine nucleobases and the ability to selectively incorporate them into an oligonucleotide through the normal phosphodiester linkage using an automated DNA synthesizer. These features should be exploited to examine critical DNA/protein interactions.

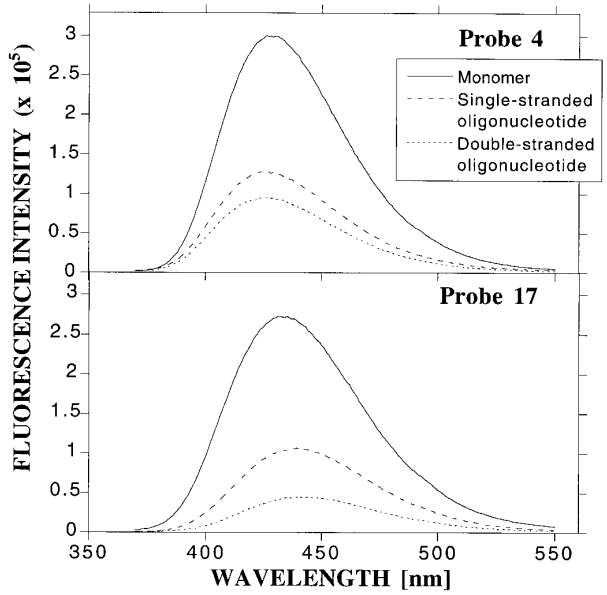

FIG. 5. Overlay of emission spectra of equimolar concentrations of probes 4 and 17 as monomer (—), and incorporated into PTER9 in single-stranded (---), and double-stranded (· · ·) forms.

TABLE 4

Melting Temperature (T_m) of Fluorophore-Containing Oligonucleotides Sequences into Which Probes 4 and 17 Were Incorporated

	T_m		
Oligonucleotide	Probe 4 (°C)	Probe 17 (°C)	Mismatch (°C)
PTER1	56.0		
PTER2	55.6		
PTER3	53.8	63.6	54.4
PTER4	52.0		54.4
PTER5	58.8	62.6	
PTER7	58.4		
PTER8	50.4	61.6	
PTER9	54.6		

Note. The site of fluorophore incorporation is shown in Table 1. T_m's were measured in 10 mM Tris, pH 7.5, with 10 mM NaCl. The T_m of double-stranded oligonucleotide containing no fluorophore was 63.2°C.

REFERENCES

1. Leonard, N. J. (1993) *CRC Crit. Rev. Biochem.* **15,** 125–199.
2. Ward, D. C., and Reich, E. (1969) *J. Biol. Chem.* **244,** 1228–1237.
3. Bloom, L. B., Otto, M. R., Beecham, J. M., and Goodman, M. F. (1993) *Biochemistry* **32,** 11247–11258.
4. Lycksell, P. O., Graslund, A., Claesens, F., McLaughlin, L. W., Larsson, U., and Rigler, R. (1987) *Nucleic Acids Res.* **15,** 9011–9025.
5. McLaughlin, L. W., Leong, T., Benseler, F., and Piel, N. (1988) *Nucleic Acids Res.* **16,** 5631–5644.
6. Nordlund, T. M., Wu, P., Andersson, S., Nilsson, L., Ribler, R., Graslund, A., McLaughlin, L. W., and Gildea, B. (1990) *SPIE Time Resolved Laser Spectrosc. Biochem. II* **1204,** 344–353.
7. Sowers, L. C., Fazakerley, G. V., Eritja, R., Kaplan, B. E., and Goodman, M. F. (1986) *Proc. Natl. Acad. Sci. USA* **83,** 5434–5438.
8. Guest, C. R., Hochstrasser, R. A., Dupuy, C. G., Allen, D. J., Benkovic, S. J., and Millar, D. P. (1991) *Biochemistry* **30,** 8759–8770.
9. Barrio, J. R., Secrist, J. A., Chien, Y.-h., Taylor, P. J., Robinson, J. L., and Leonard, N. J. (1973) *FEBS Lett.* **29,** 215–218.
10. Harris, R., and Pfleiderer, W. (1981) *Liebigs Ann. Chem.,* 1457.
11. Itoh, T., and Pfleiderer, W. (1976) *Chem. Ber.* **109,** 3228.
12. Kiriasis, W., and Pfleiderer, W. (1989) *Nucleosides Nucleotides* **8,** 1345.
13. Schmid, H., Schranner, M., and Pfleiderer, W. (1973) *Chem. Ber.* **106,** 1952.
14. Ritzmann, G., Ienaga, K., and Pfleiderer, W. (1977) *Liebigs Ann. Chem.* **1977,** 1217.
15. Ritzmann, G., and Pfleiderer, W. (1973) *Chem. Ber.* **106,** 1401.
16. Ienaga, K., and Pfleiderer, W. (1977) *Chem. Ber.* **110,** 3449.
17. Cao, C., Pfleiderer, W., Rosemeyer, H., Seela, F., Bannwarth, W., and Schonholzer, P. (1992) *Helv. Chem. Acta* **75,** 1267.
18. Lutz, H., and Pfleiderer, W. (1984) *Carbohydr. Res.* **130,** 179.
19. Ienaga, K., and Pfleiderer, W. (1977) *Chem. Ber.* **110,** 3449.

20. Hawkins, M. E., Pfleiderer, W., Mazumder, A., Pommier, Y. G., and Balis, F. M. (1995) *Nucleic Acids Res.* **23,** 2872–2880.
21. Velapoldi, R. A., and Meinenz, K. D. (1980) A Fluorescence Standard Reference Material: Quinine Sulfate Dihydrate, 260-64 National Bureau of Standards, Washington, DC.
22. Weber, G., and Tealle, F. W. J. (1967) *Trans. Faraday Soc.* **53,** 656.
23. Grinvald, A., and Steinberg, I. Z. (1974) *Anal. Biochem.* **59,** 583–598.
24. Badea, M. G., and Brand, L. (1979) *Methods Enzymol.* **61,** 378–425.
25. Knutson, J. R., Walbridge, D. G., and Brand, L. (1982) *Biochemistry* **21,** 4671–4679.
26. Chen, R. F., Knutson, J. R., Ziffer, H., and Porter, D. (1991) *Biochemistry* **30,** 5184–5195.
27. Werner, T. C., and Forster, L. S. (1979) *Photochem. Photobiol.* **29,** 905–914.
28. Koka, P., and Lee, J. (1979) *Proc. Natl. Acad. Sci. USA* **76,** 3068–3072.
29. Visser, A. J., and Lee, J. (1980) *Biochemistry* **19,** 4366–4372.
30. Davenport, L., Knutson, J. R., and Brand, L. (1986) *Faraday Discuss. Chem. Soc.* **81,** 81–94.
31. Millar, D. P., Robbins, R. J., and Zewail, A. H. (1980) *Proc. Natl. Acad. Sci. USA* **77,** 5593–5597.
32. Stryer, L., and Haugland, R. P. (1967) *Proc. Natl. Acad. Sci. USA* **58,** 719–726.